Hindawi
Journal of Nanomaterials
Volume 2021, Article ID 7165504, 12 pages
https://doi.org/10.1155/2021/7165504

Research Article

Synthesis of Carboxymethyl Chitosan-Capped Gold Nanoparticles by Gamma Irradiation with Novel Potential Applications as Antioxidant, Hepatoprotective, and Anticancer Substance

Do Thi Phuong Linh,[1,2] **Nguyen Trong Nghia**,[3] **Nguyen Thanh Vu**,[3] **Tran Le Truc Ha**,[4] **and Le Quang Luan**[3]

[1]*Institute of Malariology Parasitology and Entomology in Ho Chi Minh City, 699 Tran Hung Dao Street, District 5, Hochiminh City 700000, Vietnam*
[2]*Faculty of Biological Science, Nong Lam University, Thu Duc District, Hochiminh City 700000, Vietnam*
[3]*Biotechnology Center of Ho Chi Minh City, 2374, 1 Highway, Trung My Tay Ward, District 12, Hochiminh City 700000, Vietnam*
[4]*Nguyen Tat Thanh University, 100A Nguyen Tat Thanh, District 4, Hochiminh City 700000, Vietnam*

Correspondence should be addressed to Le Quang Luan; lequangluan@gmail.com

Received 28 April 2021; Revised 30 August 2021; Accepted 13 September 2021; Published 13 October 2021

Academic Editor: Miguel A. Correa Duarte

Gold nanoparticles capped by carboxymethyl chitosan (AuNPs/CM-chitosan) with particle sizes of 5.2–7.3 nm were successfully synthesized by the γ-irradiation of Au^{3+} solutions. Their characteristics were analysed by transmission electron microscope images, powder X-ray diffraction patterns, UV-visible spectroscopy, and Fourier transform infrared spectra. The antioxidant activity of AuNP/CM-chitosan was time dependent and much higher than that of ascorbic acid at the same concentration. On the other hand, the results of tail vein injection of AuNP/CM-chitosan in mice indicated that this product was not toxic to mice and that AuNPs were mainly distributed in liver tissue, at approximately 77.5%, 6 h after injection. The hepatoprotective activity of AuNP/CM-chitosan was also tested in acetaminophen-induced hepatotoxic mice by oral administration at daily doses of 0.5–2 mg/head. The results indicated that compared to the control, supplementation with 2 mg of AuNPs/head strongly reduced the aspartate aminotransferase and alanine aminotransferase indexes in the blood of the tested mice by approximately 66.5 and 69.3%, respectively. Furthermore, the MTT (3[4,5 dimetylthiazol-2-yl]-2,5-diphenyltetrazol bromide) assay on a liver cancer cell line (HepG2) clearly confirmed strong anticancer activity on HepG2 cells treated with 0.05–0.5 mM AuNPs and the tested cells did not survive after treatment with 0.5 mM AuNPs, while the growth of the normal cell line (L929) has no significant effect at the same treated concentration of AuNPs. The AuNP/CM-chitosan in the present study was synthesized by the γ-irradiation method without using any toxic-reducing chemical and stabilized in a natural biocompatible polymer. The strong antioxidant, hepatoprotective, and anticancer effects of this product may be supported to be used in the biomedical field.

1. Introduction

Recently, AuNPs have attracted increased attention and demonstrated promising effects and benefits in biosensor, bioimaging, and biomedical applications such as disease therapeutics, diagnostics, photothermal therapy, targeted delivery, and cancer treatment [1]. It has been shown that AuNPs can absorb light and transfer the absorbed light into thermal energy; therefore, AuNPs conjugated to cancer cells are heated by laser pulses, which can be used as a new and efficient method for the treatment of tumours [2]. AuNPs have been attached to epidermal growth factor receptor

antibodies to help them adhere strongly to cancer cells and then kill them without affecting normal cells [3]. In addition, AuNPs can be used in some methods to eliminate tumours in a short time [4]. Moreover, AuNPs were proven to possess the ability to increase the production of hepatocytes when they were denatured in association with cysteamine and added to the culture medium of liver cells [5].

There are several methods for the fabrication of AuNPs, such as radiolytic, chemical [6, 7], physical [8], and biological methods [9–11]. Among these methods, gamma ray irradiation was reported to be effective with several advantages. First, the reactions are carried out under normal conditions with high efficiency and synthesized AuNPs are highly pure and lack contamination by excessive chemical reductants and Au^{3+} ion residue. The size of AuNPs is easily controlled by varying the Au^{3+} ion or stabilizer concentration. Furthermore, the gamma ray irradiation method can be favourably applied on a large scale and the production process meets the requirements for clean production [12–14].

To date, AuNPs have been synthesized by radiation techniques using various polysaccharides for stabilization, such as dextran [15], hyaluronate [16], chitosan [13, 17], and alginate [12, 18]. Carboxymethyl chitosan (CM-chitosan), a derivative of chitosan, is a water-soluble and biocompatible polymer. This polymer possesses modulated physical and biological properties, such as sorption, moisture retention, cell function, antioxidant, antibacterial, and antiapoptotic activities. This polymer has also been used for controlled release drug delivery, pH-responsive drug delivery, and DNA delivery as a permeation enhancer [19]. Therefore, CM-chitosan is attracting increasing interest for use in applications in the biomedical and pharmaceutical fields [20]. Although CM-chitosan was reported to have several unique biological properties and has been used for stabilizing AuNPs synthesized by chemical reduction, heating, or UV-light irradiation methods [21–24], research on the synthesis of AuNPs by gamma irradiation using CM-chitosan as a stabilizer has not been carried out thus far.

The aim of the present study was at applying γ-ray (Co-60) irradiation techniques to synthesize AuNPs stabilized in CM-chitosan and to investigate their antioxidant, hepatoprotective, and anticancer activities for application as a special hepatoprotective and anticancer material.

2. Materials and Methods

2.1. Materials. Liver cancer (HepG2) and mouse fibroblast (L929) cell lines were a gift from the Animal Biotechnology Department, Biotechnology Center of Ho Chi Minh City, Vietnam. Hydrogen tetrachloroaurate ($HAuCl_4{\cdot}4H_2O$) and sodium citrate ($C_6H_5Na_3O_7{\cdot}2H_2O$) were purchased from Merck, Germany. Carboxymethyl chitosan (CM-chitosan) with Mw~30.000 was purchased from Koyo Chemical Industrial Co. Ltd., Japan. Silymarin was supplied by Sigma (USA). MTT (3[4,5 dimetylthiazol-2-yl]-2,5-diphenyltetrazol bromide) and dimethyl sulfoxide (DMSO) were purchased from Merck (Germany). ABTS (3-ethylbenzothiazoline-6-sulfonate) was supplied by Bio Basic (Canada). Acetaminophen (APAP) and other purged chemicals were purchased from Sigma (USA).

2.2. Synthesis of Gold Nanoparticles by γ-Ray Irradiation. Colloidal AuNPs with different concentrations of 0.5, 1.0, and 1.5 mM stabilized in 0.5% CM-chitosan were prepared as follows: a stock solution of 10 mM [Au^{3+}] was added to a 2% CM-chitosan solution at an appropriate ratio with deionized water and then stirred for 10 min before adjusting the pH to 7 by 1 M NaOH. Subsequently, 200 ml of prepared [Au^{3+}]/CM-chitosan solution was placed into a glass bottle with a plastic cap and irradiated at 2–10 kGy by a gamma Co-60 source (model gamma cell GC-5000, Brit, India) at the Biotechnology Center of Ho Chi Minh City with a dose rate of 10 kGy/h.

2.3. UV-vis Spectra. The UV–visible (UV-vis) spectra of the resultant AuNP colloidal solutions diluted to 0.1 mM, calculated as the [Au^{3+}] concentration using deionized water, were determined on a UV-Vis spectrophotometer (model UV-2401PC, Shimazu, Japan) [14, 25, 26].

2.4. Transmission Electron Microscope Images. The transmission electron microscope (TEM) images of AuNP samples were characterized by a JEM 1400 transmission electron microscope (TEM) (JEOL, Japan). The particle sizes and size distribution of AuNP images were determined by statistical calculation from approximately 300 particles following methods described elsewhere [25–27].

2.5. FTIR Measurement. Fourier transform infrared (FTIR) spectra of CM-chitosan and AuNP/CM-chitosan samples were obtained at ambient temperature using a Shimadzu FTIR-8100A spectrophotometer linked with a Shimadzu DR-8030 computer system. Samples were prepared in a KBr tablet formed by well-dried mixtures containing samples and KBr. All obtained spectra were the result of 128 scans at a resolution of 4 cm^{-1} in a wavelength range between 4000 and 400 cm^{-1} [21].

2.6. X-Ray Diffraction. Powder X-ray diffraction (XRD) patterns were collected at room temperature on an X'Pert PRO powder diffractometer (model XRD D8 Advance ECO, Bruker, Germany) with parafocusing Bragg-Brentano geometry using CuKα radiation ($\lambda\theta = 1.5418$ Å, $U = 40$ kV, and $I = 30$ mA). Data were scanned with the ultrafast detector X'Celerator or with a scintillator detector equipped with a secondary curved monochromator over the angular range of 5–60° (2θ) with a step size of 0.02° (2θ) and a counting time of 0.3 s $step^{-1}$. Data were evaluated by the software package HighScore Plus [16, 21].

2.7. Antioxidant Activity Test. The antioxidant activity of AuNP/CM-chitosan was investigated by using the free radical ABTS. $ABTS^{\bullet+}$ solution was prepared by mixing an equal volume of 7 mM $K_2S_2O_8$ solution with 2.45 mM ABTS solution. The solution was kept in the dark for 16 hours at room temperature. Then, the $ABTS^{\bullet+}$ solution was diluted with distilled water to obtain an optical density (OD) value of approximately 0.7 at 734 nm. To determine the antioxidant

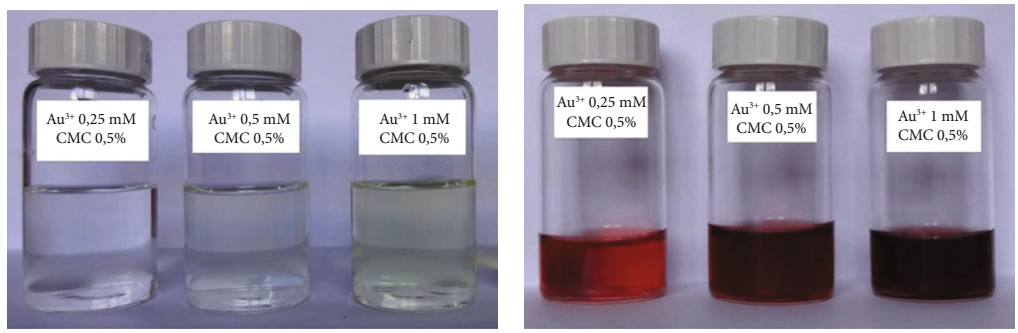

(a) (b)

Figure 1: Solutions of 0.25, 0.5, and 1.0 mM [Au^{3+}] in 0.5% CM-chitosan before (a) and after (b) irradiation at 4, 6, and 8 kGy, respectively.

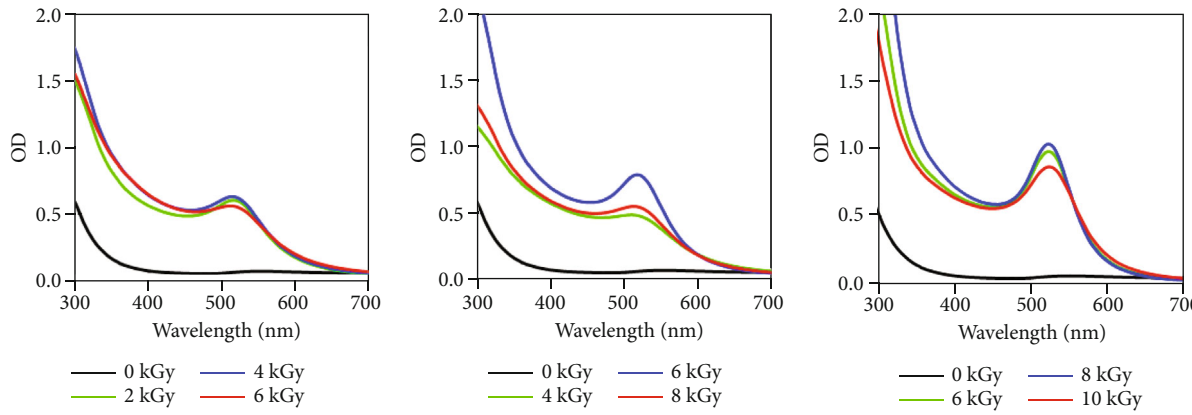

(a) (b) (c)

Figure 2: UV-vis spectra of AuNPs containing 0.25 (a), 0.5 (b) ,and 1.0 mM [Au^{3+}] (c) in 0.5% CM-chitosan irradiated at various doses.

activity of AuNPs, 2.7 ml of $ABTS^{\bullet+}$ solution was added to 0.3 ml of AuNP colloidal solution. The OD of the samples was recorded at 734 nm after 1 to 72 h. The efficiency of free radical capture was calculated based on the research of Huang et al. [28], and ascorbic acid was used as the reference [29, 30].

2.8. Investigation of the In Vivo Distribution of AuNP/CM-Chitosan in Mice. Swiss mice were supplied by the Pasteur Institute of Ho Chi Minh City and were fed at the Institute of Malariology-Parasitology-Entomology in Ho Chi Minh City for 8 weeks, and their average body weight was approximately 30 g. The mice were then injected with 0.5 ml of AuNP solution containing 1 mg of gold via the tail vein. After intravenous AuNP injection at 0, 1, 3, 6, and 12 h, the tested mice were killed to collect the liver, kidney, lung and blood. The collected tissues were then dried at 180°C for 5 h, and the content of gold in each tissue was quantitatively analysed at Dalat Nuclear Research Institute by the k_0-neutron activation analysis (k_0-NAA) method as described by Abd et al. [31].

2.9. Determination of Hepatoprotective Effects of AuNP/CM-Chitosan in Mice. Swiss mice with an average body weight of approximately 30 g were used. Ninety female mice were randomly divided into two groups (45 mice per group): the normal group and the acetaminophen- (APAP-) induced hepatotoxic group. Each group was divided into 5 tests consisting of 9 mice per test. All tested mice were then orally administered 0.2 ml of AuNP/CM-chitosan solution containing 0.5–2.0 mg of AuNPs/head once daily for 7 days. The control mice received only distilled water, while the positive control mice were supplied with silymarin at a daily dose of 2 mg/head. On day 8, all mice in the APAP-induced hepatotoxic group were orally intravenously

Table 1: The OD and λ_{max} values of AuNPs containing 0.25, 0.5, and 1.0 mM [Au^{3+}] in 0.5% CM-chitosan irradiated at various doses.

[Au^{3+}] (mM)	Irradiation dose (kGy)	λ_{max} (nm)	OD
0.25	2	507.0	0.6292
	4	510.0	0.5981
	6	515.0	0.5498
0.5	4	511.0	0.7901
	6	513.5	0.5569
	8	516.0	0.4831
1.0	6	524.0	0.8591
	8	524.0	1.0299
	10	526.0	0.9757

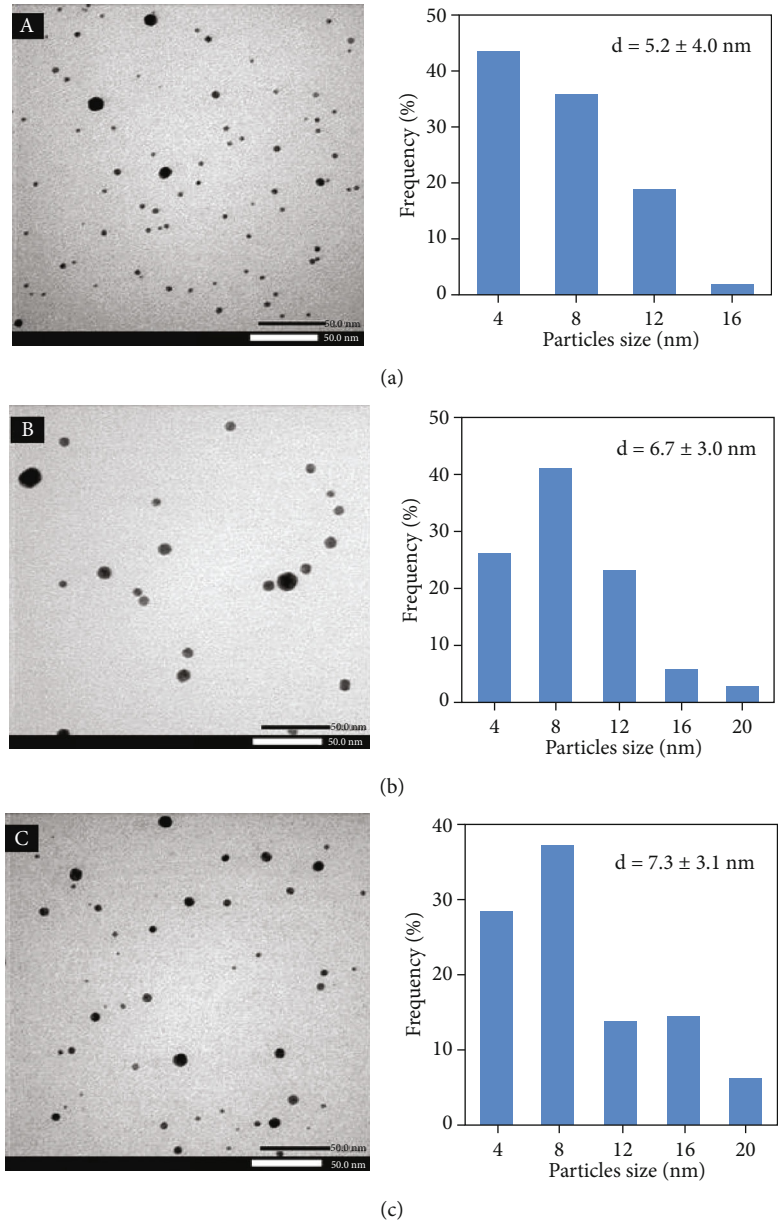

Figure 3: TEM images and size distribution of AuNPs containing 0.25 (A, a), 0.5 (B, b), and 1.0 mM [Au^{3+}] (C, c) stabilized in 0.5% CM-chitosan and prepared by γ-irradiation.

administered acetaminophen at a dose of 2000 mg/kg body weight following the method described by Das et al. [32]. After 24 h of APAP administration, 0.5 ml of blood from the myocardium of the tested mice was collected and placed into tubes containing heparin for analysis. The collected blood was then centrifuged at 4500 × g for 10 min to separate the serum [33]. The obtained serum was used to analyse aspartate aminotransferase (AST) and alanine aminotransferase (ALT) indexes on a Beckman Coulter Au480 analyser (USA). The net changes in these indexes were the average mean difference in the blood of mice before and after administration of deionized water or AuNPs.

2.10. Analysis of the Cytotoxicity of AuNP/CM-Chitosan on HepG2 and L929 Cells. MTT assays were performed with concentrations of AuNPs up to 0.5 mM to evaluate the *in vitro* cytotoxicity of liver cancer (HepG2) and mouse fibroblast (L929) cell lines. HepG2 and L929 cells were cultured in DMEM (*Dulbecco's modified Eagle medium*) containing 10% foetal bovine serum (FBS), 1% penicillin, and streptomycin at 37°C and 5% CO_2 [34]. Tested cells were plated in 96-well plates at a concentration of approximately 2×10^4 cells/well and incubated for 24 h. Consequently, cells were treated with 0.05–0.5 mM AuNPs at 37°C for 48 h in a 5% CO_2 incubator. After removal of the treated medium, the cells in each well were carefully washed with PBS (pH 7.4)

and incubated with 50 μl of MTT (0.4 mg/ml in PBS) for 4 h at 37°C and 5% CO_2. Finally, the medium was discarded before adding 100 μl of DMSO to each well to dissolve crystals. Spectrophotometrical absorbance of the purple blue formazan dye was measured by an ELISA (enzyme-linked immunosorbent assay) microplate reader at a wavelength of 570 nm (model VERSAMAX, Molecular Devices, USA). The sample without any cells served as a blank, and the toxic effect of samples on the proliferation of treated cells was determined and compared with the blank. The percentage survival of cells was determined by equation (1) as follows:

$$\text{Cell viability (\%)} = (\text{ODs/ODblank}) \times 100 \quad (1)$$

where ODs and ODblank are the absorbance of the test sample and blank sample, respectively [34, 35].

All tests in mice were conducted according to the ethical guidelines for animal research of the Institute of Malariology Parasitology and Entomology in Ho Chi Minh City, Ministry of Health of Vietnam, and followed the rules of the Declaration of Helsinki. All experiments were carried out in triplicate, and data were statistically analysed using the analysis of variance (ANOVA) test. The mean values were compared using Duncan's multiple range test with the least significant difference (LSD) at a probability level of 5%.

3. Results and Discussion

3.1. Radiation Synthesis and Characterization of AuNPs Capped by CM-Chitosan. The dose for radiation synthesis of AuNPs has been reported by Diem et al. [15]. These authors indicated that the required dose for completely reducing 1 mM [Au^{3+}] in Au^{3+}/dextran solution by gamma-ray irradiation was 6 kGy. Sun et al. [23] also informed that CM-chitosan at a concentration of 0.3–0.45% could be used as dual roles of the reducing agent and stabilizer for synthesizing AuNPs, while Ibrahim et al. [24] successfully prepared electrospun nanofibers containing AuNPs using 2% CM-chitosan. In this study, solutions with different concentrations of 0.5, 1.0, and 1.5 mM [Au^{3+}] stabilized in 0.5% CM-chitosan were irradiated by gamma-rays at doses in the range of 2–10 kGy for the synthesis of AuNPs. The results in Figure 1 show that after irradiation, the solutions containing 0.5, 1.0, and 1.5 mM [Au^{3+}] changed to a purple-red colour with optical extinction peaks (λ_{max}) at 507–526 nm (Figure 2 and Table 1). The visually changing colour is due to the characteristic surface plasmon resonance band of AuNPs after synthesis from Au^{3+} ions by irradiation [23, 24, 36, 37]. The results in Figure 2 and Table 1 also indicate that the optical extinction band intensities (OD values) of solutions containing 0.5, 1.0, and 1.5 mM [Au^{3+}] reached maximal values at irradiation doses of 4, 6, and 8 kGy, respectively. These results are in good agreement with those reported by Diem et al. [15] on the dose for completely reducing [Au^{3+}] into AuNPs by gamma-ray irradiation.

Using other natural polymer such as dextran and hyaluronate, Hien et al. [16] and Diem et al. [15] successfully prepared AuNPs with particles below 10 nm. In the present study, TEM images and corresponding histograms of particle size distributions of AuNPs in Figure 3 also showed that the AuNPs synthesized by irradiation were almost spherical. The average particle sizes of the AuNP products were found to slightly increase from 5.2 to 7.3 nm with an increasing [Au^{3+}] concentration from 0.5 to 1.5 mM.

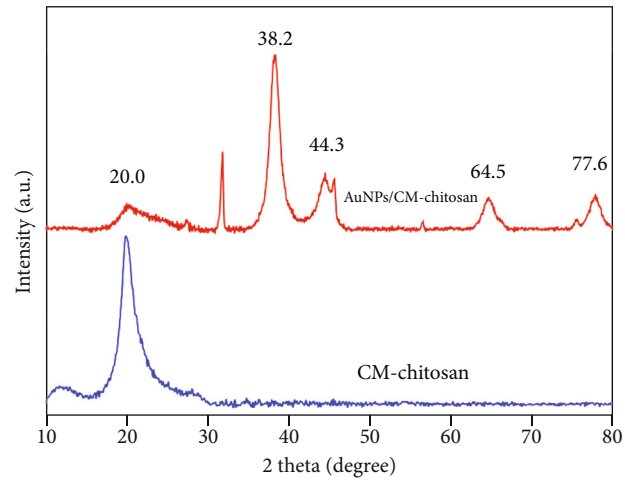

FIGURE 4: XRD pattern of CM-chitosan and AuNP-stabilized CM-chitosan.

XRD technique has been widely used for crystallization structural characterization of metal nanoparticles including AuNPs [34, 38, 39]. To further confirm the crystallization of AuNPs synthesized by γ-irradiation in this study, XRD analysis was performed with AuNP/CM-chitosan containing 1 mM [Au^{3+}]. The XRD pattern in Figure 4 clearly shows that there was only one peak at $2\theta = 20^{\circ}$ in the pattern of CM-chitosan [40–42]. In the pattern of AuNPs stabilized by CM-chitosan, four new diffraction peaks appeared at 2θ values of nearly 38.2, 44.6, 64.7, and 77.8°, corresponding to the (111), (200), (220), and (311) facets of gold, respectively. These new peaks demonstrated the presence of crystalline gold with face-centered cubic (fcc) [34, 38, 39].

FTIR analysis was also carried out to investigate the role of CM-chitosan in the stabilization of AuNPs. It can be seen clearly in Figure 5 that in the spectra of CM-chitosan, peaks appeared at 3371, 1599, 1414, 1324, and 1064 cm^{-1} assigned to O-H, C=O, N-H, N-H_2, and C-O-C linkages, respectively [21, 24]. In the spectra of AuNPs stabilized in CM-chitosan, the peaks at 3370, 1601, and 1416 cm^{-1} were shifted to longer wavelengths of 3367, 1600, and 1415 cm^{-1}, respectively. According to Huang et al. [21], these results may indicate the formation of a coordination bond between AuNPs and nitrogen/oxygen atoms in the CM-chitosan molecule.

Our characterization results for AuNPs stabilized in CM-chitosan are in good agreement with those of AuNPs synthesized by irradiation using other stabilizers, such as dextran, hyaluronate, alginate, and chitosan [12, 13, 15–18].

3.2. Antioxidant Activity of AuNPs/CM-Chitosan. Duy et al. [13] evaluated antioxidant activity of AuNPs stabilized in water-soluble chitosan with different particle sizes by free radical cation $ABTS^{\bullet+}$ scavenging method. The authors claimed that the antioxidant activity increased with the

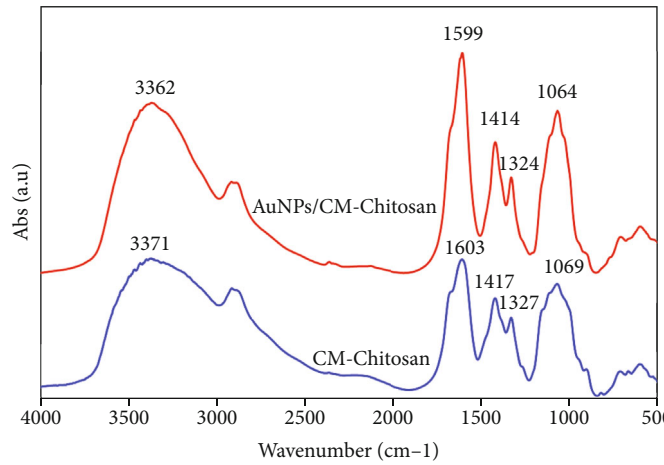

Figure 5: FTIR spectra of CM-chitosan and AuNP-stabilized CM-chitosan.

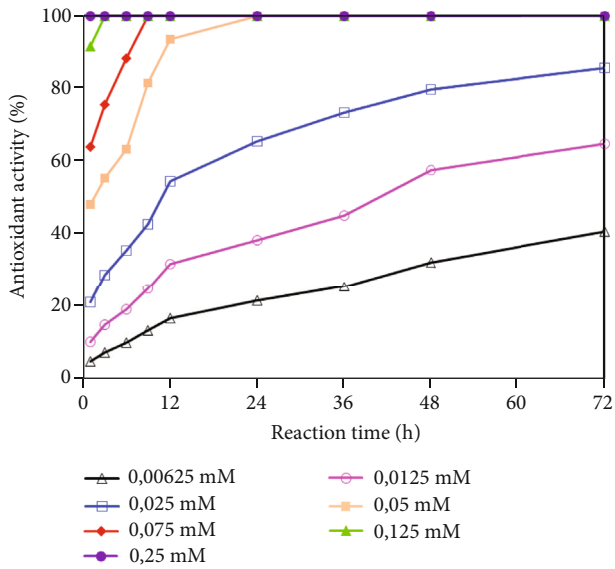

Figure 6: Antioxidant activity of AuNPs (d~7.3 nm) at different concentrations and reaction times.

increase of the reaction time and the decrease of AuNP size. The antioxidant activity of AuNP/CM-chitosan with a particle size of approximately 7.3 nm was also investigated by using the free radical ABTS method, and the obtained results in Figure 6 show that the antioxidant activity of AuNPs increased with increasing AuNP concentration. Figure 6 clearly shows that the antioxidant activities of AuNPs also increased with increasing reaction time. The reason may be due to the crystalline face-centered cubic structure of AuNPs consisting of several gold molecules, and the reaction only occurred on the surface of the particle; therefore, it may take time for all gold molecules in the nanoparticles to completely interact with free radicals [43]. This result suggests a good option for the *in vivo* application of AuNPs as antioxidant agents, especially by oral supplementation, because it will take time for AuNPs to be taken up into the blood and liver. Esumi et al. [44] reported that the antioxidant activity of AuNPs was approximately 80-fold higher than that of ascorbic acid. In this study, Figure 7 shows that the antioxidant activities after reaction of AuNPs for 72 h at concentrations ranging from 0.00625 to 0.05 mM were much higher than those of ascorbic acid at the same concentration. Since the capped chitosan derivative also contributed to the antioxidant activity, its activity was rather low compared to that of AuNP itself [13]. Therefore, the high-antioxidant activity of the AuNP/CM-chitosan may due to the small size (about 7.3 nm) of product particles. These results are in good agreement with those reported by Duy et al. [13].

3.3. In Vivo Distribution of AuNPs/CM-Chitosan in Mice. Luan et al. [12] reported that AuNPs stabilized in alginate with an average particle size of about 20 nm synthesized by gamma Co-60 irradiation were not toxic to mice at an injected dose of approximately 33.3 mg/kg body weight and the AuNP/alginate product could potentially be applied as an X-ray contrast agent, especially for the blood and liver. In this study, AuNP/CM-chitosan prepared by irradiation was injected into mice via the tail vein and the distribution in various organs was investigated to understand the *in vivo* distribution of this AuNP product. After injection, the content of AuNPs in the blood, liver, kidney, and lung tissues of mice was analysed at 1, 3, 6, 9, and 12 h postinjection. The results in Figure 8 indicated that in blood tissue, the AuNP content decreased with postinjection time and almost disappeared at 6 h postinjection (0.004 mg/g tissue). Figure 8 also shows that 1 h after injection, AuNPs started penetrating into the liver, kidney, and lung tissues and were mainly concentrated in the liver and lung tissue 6 h after injection. In particular, the gold content in liver tissue was approximately 0.775 mg/g tissue (comprising approximately 77.5% of the injected dose), while the content in lung tissue was approximately 0.075 mg/g tissue (approximately 7.5% of the injected dose). The gold content in kidney tissue was quite low (0.018 mg mg/g tissue, comprising only approximately 1.8% of the injected dose) compared to those in liver and lung tissues. Twelve hours after injection, the gold content in liver tissue was reduced to 0.467 mg/g tissue (comprising approximately 46.7% of the injected dose), while this content was almost unchanged in lung (0.076 mg/g

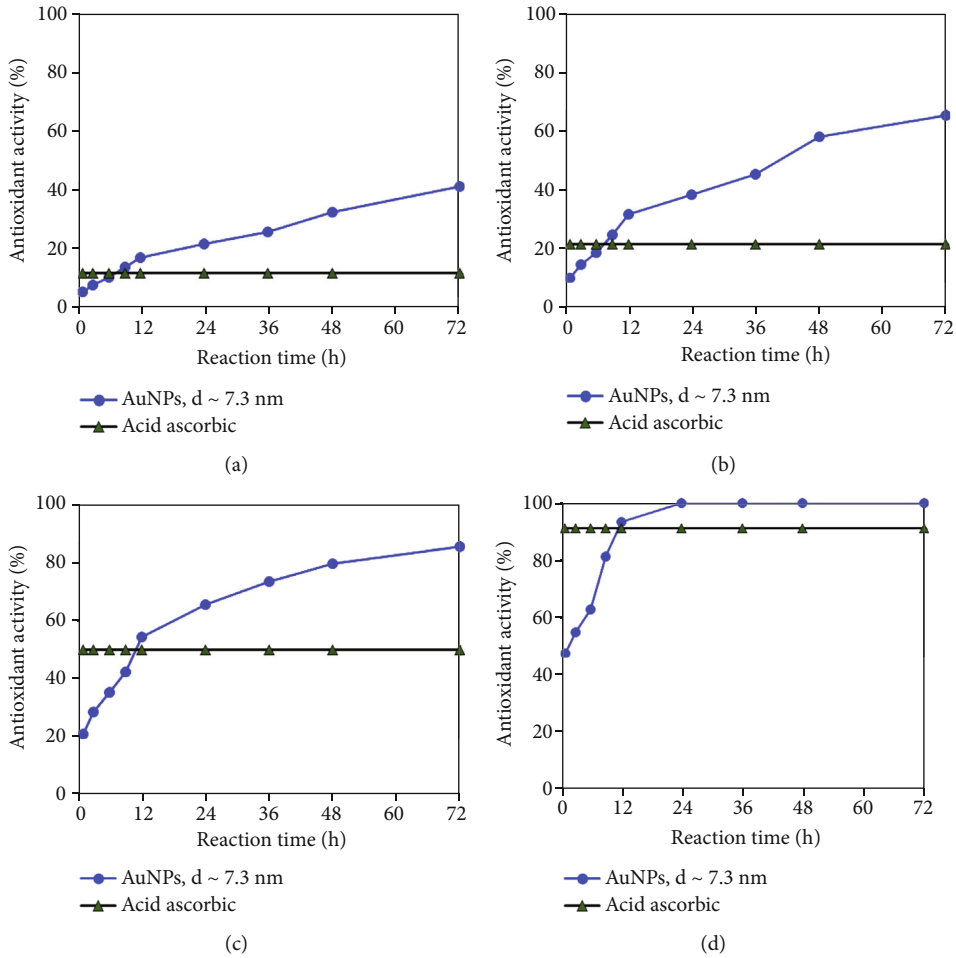

FIGURE 7: Comparison of the antioxidant activity after reaction for 72 h between AuNPs (d~7.3 nm) and ascorbic acid at the same concentrations of 0.00625 (a), 0.0125 (b), 0.025 (c), and 0.05 mM (d).

tissue) and kidney tissues (0.012 mg/g tissue). It can also be seen in Figure 8 that after injection, AuNPs were transferred from blood tissue into other organs and mostly accumulated in the liver and lung, with maximal accumulation found at 6 h post injection. A kinetic study was performed by Jong et al. [45] to determine the influence of the particle size on the *in vivo* tissue distribution of spherical-shaped AuNPs in the rat. They concluded that AuNPs with a size about 10 nm in aqueous solution concentrated mainly in the liver at 24 h after intravenous injection. In addition, Luan et al. [12] also reported that AuNPs/alginate with a particle size about 20 nm penetrated with 76.33% in the liver of mice at 6 h post injection. It seems that the *in vivo* distribution of AuNPs was affected by its particle size. In the present study, AuNPs with a size about 7.3 nm were used and the obtained results are in good agreement with those of previous reports [12, 45]. These results also suggest the appropriate application of AuNPs as hepatoprotective and liver anticancer agents.

3.4. The In Vivo Hepatoprotective Activity of AuNP/CM-Chitosan in Mice. Wang et al. [46] reported that AuNPs with particle sizes in the range of 5–70 nm were not toxic to human skin cells. In addition, the results from Pokharkar et al. [47] indicated that the LD_{50} value for oral administration of AuNPs stabilized in chitosan in rats was more than 2000 mg/kg. These authors concluded that AuNPs/chitosan produced no toxicity in rats and could be exploited for potential therapeutic applications. Furthermore, a study on the *in vivo* toxicity of 15 nm AuNPs capped by bovine serum albumin (BSA) via tail vein injection by Nghiem et al. [48] also proved that the tail vein injection of AuNPs at a dose up to 5.84 mg/kg did not cause any mortality or gross behavioural changes in tested mice. On the other hand, Negahdary et al. [49] demonstrated that AuNPs with a particle size of approximately 10 nm reduced the CAT and GPX indexes in Wistar mice. The hepatoprotective activity of AuNP/CM-chitosan was also tested in Swiss mice by oral supplementation with a daily dose from 0.5 to 2.0 mg of AuNPs/head. The AST and ALT indexes in the blood of the tested mice were analysed after 7 days of daily supplementation. The effect of AuNPs on the AST index in the blood of mice is shown in Figure 9. After 7 days of supplementation with AuNPs at concentrations of 0.5–2.0 mg/head, the AST index in the blood of both normal mice and APAP-induced hepatotoxic mice was decreased.

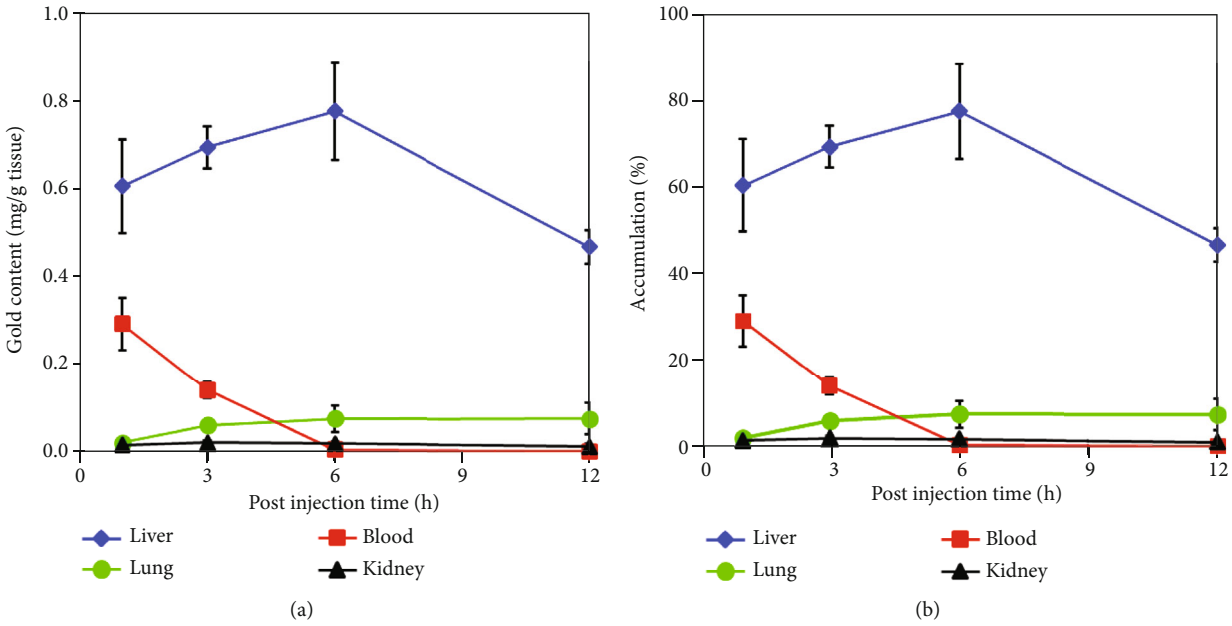

FIGURE 8: The *in vivo* accumulation content (a) and distribution ratio (b) of AuNPs (d~7.3 nm) in different tissues of mice after intravenous injection with a dose of 1 mg of AuNPs per mouse.

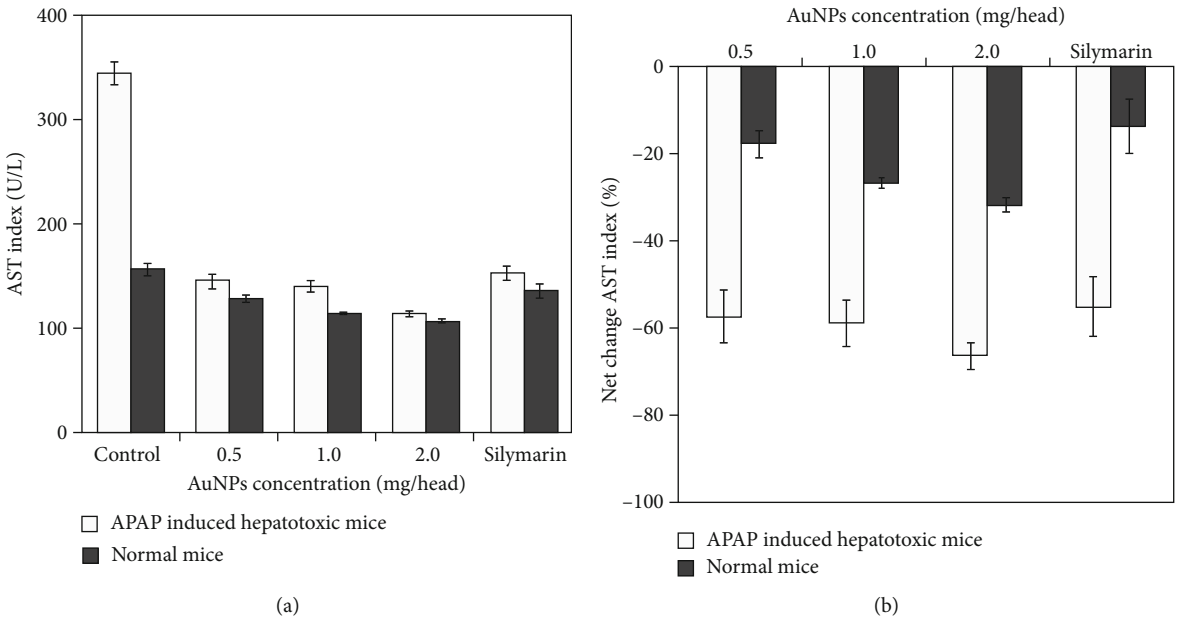

FIGURE 9: AST index (a) and the net change in this index (b) in the blood of tested mice after 7 days of oral administration of AuNPs at various daily doses.

The results in Figure 9 show that AST indexes in the blood of normal mice and the APAP-induced hepatotoxic group were in the ranges of 107.5–157.6 U/L and 115.3–344.4 U/L (Figure 9(a)), respectively. The reduction in this index was found to be directly proportional to the supplemented concentration of AuNPs. In the normal group, the maximum reduction in AST was found in the blood of only approximately 31.7% of mice supplemented with a daily dose of 2 mg of AuNPs/head. The maximum reduction in this index in the blood of APAP-induced hepatotoxic mice supplemented with 2 mg of AuNPs/head was approximately 66.5% (compared to the APAP-induced hepatotoxic mice supplemented with only distilled water). In the blood of mice supplemented with silymarin (positive control mice), the net change in the AST index was found to be similar to that of mice supplemented with 0.5–1 mg of AuNPs/head (Figure 9(b)).

On the other hand, the oral administration of AuNP products lowered the AST index in the blood of both the normal and APAP-induced hepatotoxic groups

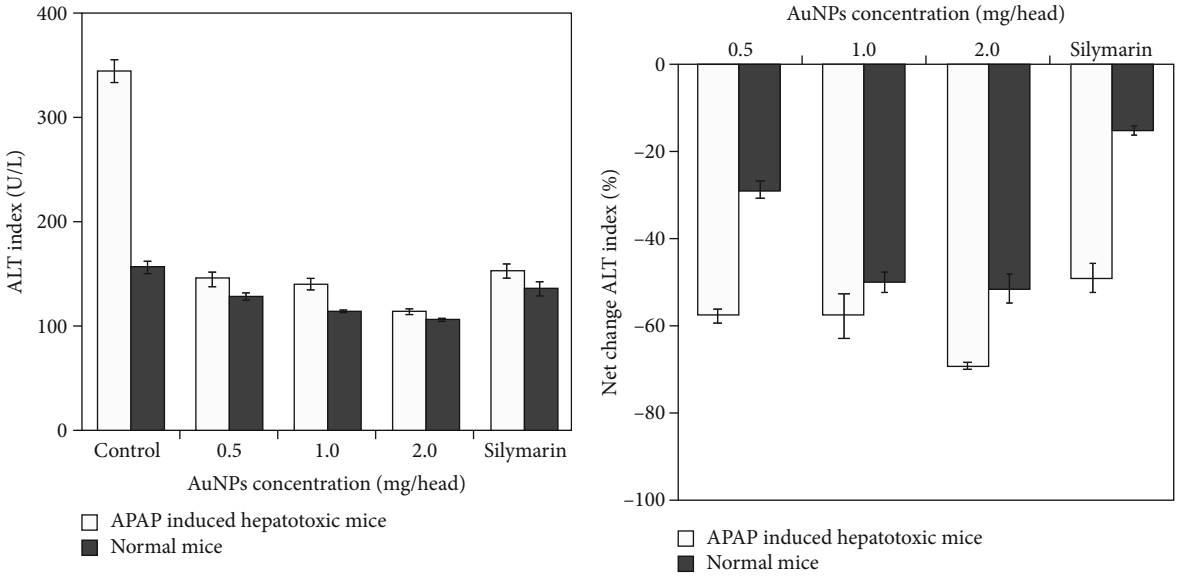

Figure 10: ALT index (a) and the net change in this index (b) in the blood of tested mice after 7 days of oral administration of AuNPs at various daily doses.

(Figure 10(a)). For the normal group, AuNP supplementation with daily doses of 0.5–2 mg per mouse reduced the AST index by approximately 29.1–51.6% (compared to that in the blood of control mice) (Figure 10(b)). The net change in this index in the blood of mice supplemented with silymarin (the positive control) was only 15%. In the case of APAP-induced hepatotoxic groups, the results from Figure 10(b) also showed that oral supplementation with AuNPs at daily doses of 0.5–2 mg/head reduced the ALT index to 57.7–69.3%. The net change in ALT in the blood of positive control mice supplemented with silymarin was similar to that in the blood of mice supplemented with 0.5–1.0 mg/head but far lower than that in the blood of mice orally administered a daily dose of 2 mg/head. It can be seen clearly in Figures 6–8 that the AuNPs stabilized in CM-chitosan and synthesized by gamma Co-60 irradiation displayed strong antioxidant activity and the *in vivo* distribution of this product was mainly in liver tissue. These results may be the main reason for the reduction in the AST and ALT indexes in the blood of the tested mice.

3.5. In Vitro Cytotoxicity of AuNP/CM-Chitosan on Liver Cancer (HepG2) and Mouse Fibroblast (L929) Cell Lines. Biosynthesized AuNPs have been reported to have cytotoxic effects on various cancer cell lines, such as PA1 (human ovarian cancer cell line), MCF7 (breast cancer cell line), A549 (lung cancer cell line), and HepG2 [50–52]. Even so, the cytotoxicity of AuNPs synthesized by gamma irradiation on cancer cell lines is still limited. In the present study, the anticancer activity of AuNPs was tested *in vitro* using the HepG2 cell line. The anticancer activity of AuNP/CM-chitosan against the HepG2 cell line was carried out at concentrations in the range of 0.05–0.5 mM. In the MTT assay, the anticancer effect of AuNP concentration on HepG2 cell lines was evaluated via the cell viability percentage. Figure 11

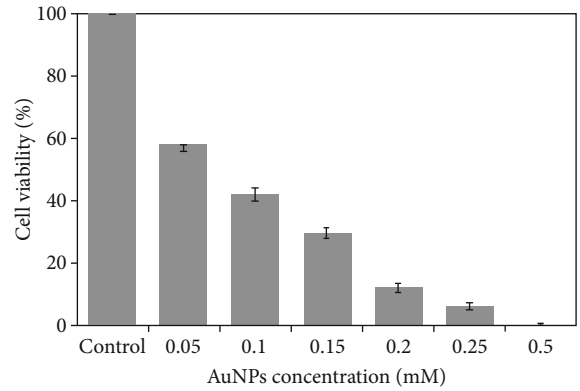

Figure 11: Anticancer activity of AuNPs against HepG2 cells.

shows that the viability of HepG2 cells was decreased by increasing the AuNP concentration. This means that the anticancer activity of AuNPs against HepG2 cells was directly proportional to the concentration of the AuNP product. Compared to the control (without AuNP treatment), the survival rates of HepG2 cells were decreased from 57.9 to 12.2% by treatment with AuNPs at concentrations ranging from 0.05 to 0.2 mM. The viability of this cell line was only approximately 5.9% after the addition of 0.25 mM AuNPs. After treatment with 0.5 mM AuNPs, HepG2 cells did not survive. AuNPs have reported to show a significant inhibition on the growth of HepG2 cells at the concentration of 50–250 mg/l [50, 51]. Li et al. [34] demonstrated that AuNPs stabilized in plant-based extract strongly inhibited the viability of HepG2 liver carcinoma cells at the concentration of 50–100 mg/l. The treatment of this AuNP product to HepG2 cells reduced the expressions of antiapoptotic proteins (Bcl-XL and Bcl-2) and improved the expressions of proapoptotic protein (Bax, caspase-3, and caspase-9). While

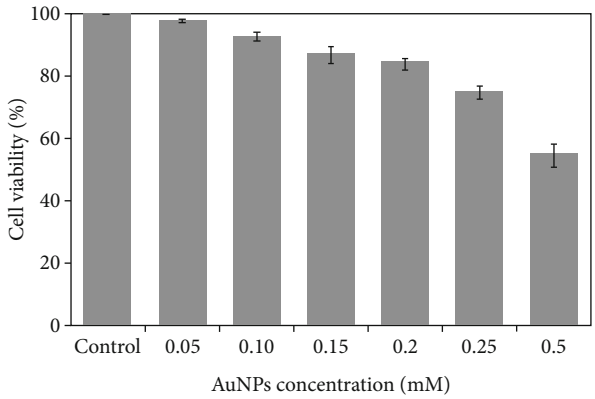

Figure 12: Cytotoxicity effect of AuNPs on L929 cells.

Lopez-Chaves et al. [53] reported that the deleterious effect of AuNPs on HepG2 cells was due to reactive oxygen species (ROS) production and DNA damage. The authors also mentioned that the smaller size of AuNPs could induce a stronger cytotoxicity effect on the HepG2 cell line. Our results are in good agreement with those reported in previous papers [34, 50, 51, 53].

On the other hand, the cytotoxicity of AuNPs were also evaluated on normal cells including L929 cell line mouse fibroblast [54, 55]. Pattanayak et al. [54] informed that AuNPs capped with β-D glucan did not exhibit any cytotoxicity on normal cell (mouse fibroblast L929 cell line) at the treated concentration unto 1000 mg/l. Raju et al. [55] also reported that the treatment of the L929 cell line with 1.1–1% AuNPs capped with citrate had no effect on the growth and viability of treated cells. In this study, the cytotoxicity of AuNP/CN-chitosan was also tested on the L929 cell line. The results in Figure 12 indicate that the cell viability of the normal cell line was significantly decreased by the treated AuNP concentration from 0.01 to 0.25 mM. However, the L929 cell viability decreased to 54.5% at the treated AuNP concentration of 0.5 mM. These results clearly revealed that AuNP/CN-chitosan synthesized by the γ-irradiation method had a low cytotoxicity effect in normal cell.

4. Conclusions

AuNPs with particle sizes of 5.3 - 7.2 nm capped in CM-chitosan were successfully synthesized by the γ-irradiation method. The antioxidant activity of AuNP/CM-chitosan prepared by radiation was much stronger than that of ascorbic acid at the same concentration. The intravenous administration test indicated that the AuNP/CM-chitosan product was not toxic to mice and AuNPs were mainly distributed in liver tissue (approximately 77.5%) after injection. The oral administration trial with a daily dose of 2 mg/head for mice also confirmed a strong reduction effect of AuNP/CM-chitosan on the AST (66.5%) and ALT (69.3%) indexes in APAP-induced hepatotoxicity. Additionally, the present study clearly showed strong anticancer activity of AuNPs on the HepG2 cell line and the tested liver cancer cells could not survive treatment with 0.5 mM AuNPs. While the treatment of this product at concentrations up to 0.5 mM did not show any significant inhibition on the growth of normal cell line (mouse fibroblast L929 cell). The radiation-synthesized AuNP/CM-chitosan product may potentially be used as an antioxidant, hepatoprotective, and liver anticancer agent in nutraceutical food production, cosmetics, and/or biomedicine.

Data Availability

The data will be available upon request to the corresponding author.

Conflicts of Interest

The authors declare that they have no conflict of interest.

Acknowledgments

The authors would like to thank the Biotechnology Center of Ho Chi Minh City for their financial support.

References

[1] S. Bharathiraja, P. Manivasagan, N. Quang Bui et al., "Cytotoxic induction and photoacoustic imaging of breast cancer cells using astaxanthin-reduced gold nanoparticles," *Nanomaterials*, vol. 6, no. 4, p. 78, 2020.

[2] X. Huang and M. A. El-Sayed, "Gold nanoparticles: optical properties and implementations in cancer diagnosis and photothermal therapy," *Journal of Advanced Research*, vol. 1, no. 1, pp. 13–28, 2010.

[3] C. R. Patra, R. Bhattacharya, D. Mukhopadhyay, and P. Mukherjee, "Fabrication of gold nanoparticles for targeted therapy in pancreatic cancer," *Advanced Drug Delivery Reviews*, vol. 62, no. 3, pp. 346–361, 2010.

[4] I. H. El-Sayed, X. Huang, and M. A. El-Sayed, "Selective laser photo-thermal therapy of epithelial carcinoma using anti-EGFR antibody conjugated gold nanoparticles," *Cancer Letter*, vol. 239, no. 1, pp. 129–135, 2006.

[5] H. Y. Gu, Z. Chen, R. X. Sa et al., "The immobilization of hepatocytes on 24 nm-sized gold colloid for enhanced hepatocytes proliferation," *Biomaterials*, vol. 25, no. 17, pp. 3445–3451, 2004.

[6] A. Gautam, G. P. Singh, and S. Ram, "A simple polyol synthesis of silver metal nanopowder of uniform particles," *Synthetic Metals*, vol. 157, no. 1, pp. 5–10, 2007.

[7] S. Clichici, L. David, B. Moldovan et al., "Hepatoprotective effects of silymarin coated gold nanoparticles in experimental cholestasis," *Materials Science and Engineering: C*, vol. 115, article 111117, 2020.

[8] A. V. Simakin, V. V. Voronov, G. A. Shafeev, R. Brayner, and F. Bozon-Verduraz, "Nanodisks of Au and Ag produced by laser ablation in liquid environment," *Chemical Physics Letters*, vol. 348, no. 3-4, pp. 182–186, 2001.

[9] S. Sinha, I. Pam, P. Chanda, and S. K. Sen, "Nanoparticles fabrication using ambient biological resources," *Journal of Applied Bioscience*, vol. 19, pp. 1113–1130, 2009.

[10] M. S. Nejad, G. H. S. Bonjar, and N. Khaleghi, "Biosynthesis of gold nanoparticles using *Streptomyces fulvissimus*," *Nanomedicine Journal*, vol. 2, no. 2, pp. 153–159, 2015.

[11] T. T. Vo, T. T. N. Nguyen, T. T. T. Huynh et al., "Biosynthesis of Silver and Gold Nanoparticles Using Aqueous Extract from Crinum latifolium Leaf and Their Applications Forward Antibacterial Effect and Wastewater Treatment," *Journal of Nanomaterials*, vol. 2019, Article ID 8385935, 14 pages, 2019.

[12] Q. L. le, T. P. Linh Do, H. P. U. Nguyen, V. P. Dang, and Q. H. Nguyen, "Biodistribution of gold nanoparticles synthesized byγ-irradiation after intravenous administration in mice," *Advances in Natural Sciences: Nanoscience and Nanotechnology*, vol. 5, no. 2, article 025009, 2014.

[13] N. N. Duy, D. X. du, D. van Phu, L. A. Quoc, B. D. du, and N. Q. Hien, "Synthesis of gold nanoparticles with seed enlargement size by γ-irradiation and investigation of antioxidant activity," *Colloids and Surfaces A: Physicochemical and Engineering Aspects*, vol. 436, pp. 633–638, 2013.

[14] P. Chen, L. Song, Y. Liu, and Y. Fang, "Synthesis of silver nanoparticles by γ -ray irradiation in acetic water solution containing chitosan," *Radiation Physics and Chemistry*, vol. 76, no. 7, pp. 1165–1168, 2007.

[15] P. H. N. Diem, D. T. T. Thao, D. V. Phu et al., "Synthesis of gold nanoparticles stabilized in dextran solution by gamma Co-60 ray irradiation and preparation of gold nanoparticles/-dextran powder," *Journal of Chemistry*, vol. 2017, Article ID 6836375, 8 pages, 2017.

[16] N. Q. Hien, D. van Phu, N. N. Duy, and L. A. Quoc, "Radiation synthesis and characterization of hyaluronan capped gold nanoparticles," *Carbohydrate Polymers*, vol. 89, no. 2, pp. 537–541, 2012.

[17] K. D. N. Vo, C. Kowandy, L. Dupont, C. Coqueret, and N. Q. Hien, "Radiation synthesis of chitosan stabilized gold nanoparticles comparison between e^- beam and γ irradiation," *Radiation Physics and Chemistry*, vol. 94, pp. 84–87, 2014.

[18] N. Tue Anh, D. van Phu, N. Ngoc Duy, B. Duy du, and N. Quoc Hien, "Synthesis of alginate stabilized gold nanoparticles by γ-irradiation with controllable size using different Au^{3+} concentration and seed particles enlargement," *Radiation Physics and Chemistry*, vol. 79, no. 4, pp. 405–408, 2010.

[19] V. K. Mourya, N. N. Inamdar, and A. Tiwari, "Carboxymethyl chitosan and its applications," *Advanced Materials Letters*, vol. 1, no. 1, pp. 11–33, 2010.

[20] Z. Shariatinia, "Carboxymethyl chitosan: properties and biomedical applications," *International Journal of Biological Macromolecules*, vol. 120, no. 2018, pp. 1406–1419, 2018.

[21] L. Huang, M. Zhai, J. Peng, L. Xu, J. Li, and G. Wei, "Synthesis, size control and fluorescence studies of gold nanoparticles in carboxymethylated chitosan aqueous solutions," *Journal of Colloid and Interface Science*, vol. 316, no. 2, pp. 398–404, 2007.

[22] M. J. Laudenslager, J. D. Schiffman, and C. L. Schauer, "Carboxymethyl chitosan as a matrix material for platinum, gold, and silver nanoparticles," *Biomacromolecules*, vol. 9, no. 10, pp. 2682–2685, 2008.

[23] L. Sun, S. Pu, J. Li et al., "Size controllable one step synthesis of gold nanoparticles using carboxymethyl chitosan," *International Journal of Biological. Macromolecules*, vol. 122, no. 2019, pp. 770–783, 2019.

[24] H. M. Ibrahim, M. M. Reda, and A. Klingner, "Preparation and characterization of green carboxymethylchitosan (CMCS) - Polyvinyl alcohol (PVA) electrospun nanofibers containing gold nanoparticles (AuNPs) and its potential use as biomaterials," *International Journal of Biological Macromolecules*, vol. 151, no. 2020, pp. 821–829, 2020.

[25] T. Li, H. G. Park, and S. H. Choi, "Γ-irradiation-induced preparation of Ag and Au nanoparticles and their characterizations," *Materials Chemistry and Physics*, vol. 105, no. 2-3, pp. 325–330, 2007.

[26] D. V. Phu, V. T. K. Lang, N. T. Kim Lan et al., "Synthesis and antimicrobial effects of colloidal silver nanoparticles in chitosan byγ-irradiation," *Journal of Experimental Nanoscience*, vol. 5, no. 2, pp. 169–179, 2010.

[27] S. Aryal, K. C. Remant Bahadur, M. S. Khil, N. Dharmaraj, and H. Y. Kim, "Radical scavenger for the stabilization of gold nanoparticles," *Materials Letters*, vol. 61, no. 19-20, pp. 4225–4230, 2007.

[28] B. Huang, X. Ban, J. He, J. Tong, J. Tian, and Y. Wang, "Hepatoprotective and antioxidant activity of ethanolic extracts of edible lotus (*Nelumbo nucifera* Gaertn.) leaves," *Food Chemistry*, vol. 120, no. 3, pp. 873–878, 2010.

[29] R. Re, N. Pellegrini, A. Proteggente, A. Pannala, M. Yang, and C. Rice-Evans, "Antioxidant activity applying an improved ABTS radical cation decolorization assay," *Free Radical Biology and Medicine*, vol. 26, no. 9-10, pp. 1231–1237, 1999.

[30] K. Thaipong, U. Boonprakob, K. Crosby, L. Cisneros-Zevallos, and D. Hawkins Byrne, "Comparison of ABTS, DPPH, FRAP, and ORAC assays for estimating antioxidant activity from guava fruit extracts," *Journal of Food Composition and Analysis*, vol. 19, no. 6-7, pp. 669–675, 2006.

[31] A. E. Abd, M. Hamdy, M. Mostafa, and M. El-Amir, "Application of K_0-NAA in the determination of gold and other trace elements in mineralized rocks from El-Sid gold district, Eastern Desert, Egypt," *Journal of Nuclear and Radiation Physics*, vol. 4, no. 1, pp. 21–29, 2009.

[32] J. Das, J. Ghosh, P. Manna, and P. C. Sil, "Taurine protects acetaminophen-induced oxidative damage in mice kidney through APAP urinary excretion and CYP2E1 inactivation," *Toxicology*, vol. 269, no. 1, pp. 24–34, 2010.

[33] N. T. Long, N. T. N. Anh, B. L. Giang, H. N. Son, and L. Q. Luan, "Radiation degradation of β-glucan with a potential for reduction of lipids and glucose in the blood of mice," *Polymers*, vol. 11, no. 6, article 955, 2019.

[34] L. Li, W. Zhang, V. D. Desikan Seshadri, and G. Cao, "Synthesis and characterization of gold nanoparticles fromMarsdenia tenacissimaand its anticancer activity of liver cancer HepG2 cells," *Artificial Cells, Nanomedicine, And Biotechnology*, vol. 47, no. 1, pp. 3029–3036, 2019.

[35] A. Zerboni, R. Bengalli, G. Baeri, L. Fiandra, T. Catelani, and P. Mantecca, "Mixture effects of diesel exhaust and metal oxide nanoparticles in human lung A549 cells," *Nanomaterials*, vol. 9, no. 9, article 1302, 2019.

[36] M. Shen, Y. du, N. Hua, and N. Yang, "Microwave irradiation synthesis and self-assembly of alkylamine-stabilized gold nanoparticles," *Powder Technology*, vol. 162, no. 1, pp. 64–72, 2006.

[37] Y. Luo, "Size-controlled preparation of dendrimer-protected gold nanoparticles: A sunlight irradiation-based strategy," *Materials Letters*, vol. 62, no. 21-22, pp. 3770–3772, 2008.

[38] A. Madhusudhan, G. B. Reddy, M. Venkatesham et al., "Efficient pH dependent drug delivery to Target cancer cells by gold nanoparticles capped with carboxymethyl chitosan," *International Journal of Molecular Sciences*, vol. 15, no. 5, pp. 8216–8234, 2014.

[39] B. Sundararajan and B. D. Ranjitha Kumari, "Novel synthesis of gold nanoparticles using *Artemisia vulgaris* L. leaf extract

and their efficacy of larvicidal activity against dengue fever vector *Aedes aegypti* L.," *Journal of Trace Elements in Medicine and Biology*, vol. 43, pp. 187–196, 2017.

[40] R. K. Farag and R. R. Mohamed, "Synthesis and characterization of carboxymethyl chitosan nanogels for swelling studies and antimicrobial activity," *Molecules*, vol. 18, no. 1, pp. 190–203, 2013.

[41] X. Yan, Z. Tong, Y. Chen et al., "Bioresponsive materials for drug delivery based on carboxymethyl chitosan/poly(γ-glutamic acid) Composite microparticles," *Marine Drugs*, vol. 15, no. 5, p. 127, 2017.

[42] Q. K. Zhong, Z. Y. Wu, Y. Q. Qin et al., "Preparation and properties of carboxymethyl chitosan/alginate/tranexamic acid Composite films," *Membranes*, vol. 9, no. 1, article 11, 2019.

[43] N. O. Yakimovich, A. A. Ezhevskii, D. V. Guseinov, L. A. Smirnova, T. A. Gracheva, and K. S. Klychkov, "Antioxidant properties of gold nanoparticles studied by ESR spectroscopy," *Russian Chemical Bulletin*, vol. 57, no. 3, pp. 520–523, 2008.

[44] K. Esumi, N. Takei, and T. Yoshimura, "Antioxidant-potentiality of gold-chitosan nanocomposites," *Colloids and Surfaces B: Biointerfaces*, vol. 32, no. 2, pp. 117–123, 2003.

[45] W. H. de Jong, W. I. Hagens, P. Krystek, M. C. Burger, A. J. A. M. Sips, and R. E. Geertsma, "Particle size-dependent organ distribution of gold nanoparticles after intravenous administration," *Biomaterials*, vol. 29, no. 12, pp. 1912–1919, 2008.

[46] S. Wang, W. Lu, O. Tovmachenko, U. S. Rai, H. Yu, and P. C. Ray, "Challenge in understanding size and shape dependent toxicity of gold nanomaterials in human skin keratinocytes," *Chemical Physics Letters*, vol. 463, no. 1-3, pp. 145–149, 2008.

[47] V. Pokharkar, S. Dhar, D. Bhumkar, V. Mali, S. Bodhankar, and B. L. V. Prasad, "Acute and subacute toxicity studies of chitosan reduced gold nanoparticles: a novel carrier for therapeutic agents," *Journal of Biomedical Nanotechnology*, vol. 5, no. 3, pp. 233–239, 2009.

[48] T. H. Lien Nghiem, T. T. Nguyen, E. Fort et al., "Capping andin vivotoxicity studies of gold nanoparticles," *Advances in Natural Sciences: Nanoscience and Nanotechnology*, vol. 3, no. 1, article 015002, 2012.

[49] M. Ajdary, M. Negahdary, R. Chelongar, and S. K. zadeh, "The antioxidant effects of silver, gold, and zinc oxide nanoparticles on male mice in *In Vivo* condition," *Advanced Biomedical Research*, vol. 4, no. 1, p. 69, 2015.

[50] T. Muthukumar, B. Sudhakumari, A. Sambandam, T. Aravinthan, P. Sastry, and J. H. Kim, "Green synthesis of gold nanoparticles and their enhanced synergistic antitumor activity using HepG2 and MCF7 cells and its antibacterial effects," *Process Biochemistry*, vol. 51, no. 3, pp. 384–391, 2016.

[51] S. Rajeshkumar, "Anticancer activity of eco-friendly gold nanoparticles against lung and liver cancer cells," *Journal of Genetic Engineering and Biotechnology*, vol. 14, no. 1, pp. 195–202, 2016.

[52] R. Maity, M. Chatterjee, A. Banerjee et al., "Gold nanoparticle-assisted enhancement in the anti-cancer properties of theaflavin against human ovarian cancer cells," *Materials Science and Engineering C*, vol. 104, article 109909, 2019.

[53] C. Lopez-Chaves, J. Soto-Alvaredo, M. Montes-Bayon, J. Bettmer, J. Llopis, and C. Sanchez-Gonzalez, "Gold nanoparticles: Distribution, bioaccumulation and toxicity. *In vitro* and *in vivo* studies," *Nanomedicine: Nanotechnology, Biology, and Medicine*, vol. 14, no. 1, pp. 1–12, 2018.

[54] S. Pattanayak, S. Chakraborty, S. Biswas, D. Chattopadhyay, and M. Chakraborty, "Degradation of methyl parathion, a common pesticide and fluorescence quenching of rhodamine B, a carcinogen using β-D glucan stabilized gold nanoparticles," *Journal of Saudi Chemical Society*, vol. 22, no. 8, pp. 937–948, 2018.

[55] G. Raju, N. Katiyar, S. Vadukumpully, and S. A. Shankarappa, "Penetration of gold nanoparticles across the stratum corneum layer of thick- Skin," *Journal of Dermatological Science*, vol. 89, no. 2, pp. 146–154, 2018.